


 Cite this: *RSC Adv.*, 2025, **15**, 25542

 Received 25th June 2025  
 Accepted 8th July 2025

DOI: 10.1039/d5ra04525h

[rsc.li/rsc-advances](http://rsc.li/rsc-advances)

# Muhenrins A–C, pimarane-type diterpenoids from *Munronia henryi*†

Wan-Bai Su, Xiao-Meng Hou, Ling Zhang, Li Yan, Zhi-Yang Tang, Yang Yu, Jin-Song Liu, Yun-Peng Sun\* and Guo-Kai Wang\*

Three undescribed pimarane-type diterpenoids, muhenrins A–C (1–3), along with a known analogue were isolated from the petroleum ether extract of *Munronia henryi* (Meliaceae). Their structures, including absolute configurations, were elucidated by means of various spectroscopic methods (IR, UV, HR-ESI-MS, NMR), single-crystal X-ray diffraction, ECD and NMR calculations. Muhenrin A (1) features a unique 6,7-*seco* pimarane skeleton, and its putative biosynthetic pathways have been proposed. Compounds 1–4 showed weak inhibitory activity against NO production in LPS-induced RAW 264.7 cells, with inhibition rates ranging from 13.73 – 32.35% at 50  $\mu$ M concentrations.

## Introduction

The plant genus *Munronia* (Meliaceae) comprises approximately 15 species, primarily distributed in China, Sri Lanka, India, Indonesia, and the Philippines. Among them, about 7–8 species native to China and is traditionally utilized in folk medicine, particularly among ethnic minorities.<sup>1</sup> The whole herb of *Munronia* is widely employed to treat malaria, rheumatic joint pain, coughs, stomachaches, and has demonstrated notable insecticidal activity.<sup>2</sup> Although the medicinal value of *Munronia* plants has been documented in numerous ethnic medical classics, scientific data on their chemical composition and pharmacological effects remain limited. Current studies reveal that *Munronia* species are rich in limonoids and triterpenoids,<sup>2–5</sup> which exhibit notable biological activities, including anti-inflammatory,<sup>6</sup> anti-tumor,<sup>2</sup> anti-TMV (tobacco

mosaic virus),<sup>4</sup> and anti-proliferative effects.<sup>5</sup> Our research group previously isolated 74 limonoids, 4 triterpenoids, and 2 pregnanes from *Munronia unifoliolata* Oliv.<sup>6–8</sup> Among these, munronoid I demonstrated significant anti-inflammatory activity by markedly suppressing IL-1 $\beta$  release through inhibition of NLRP3 inflammasome initiation and assembly.<sup>6</sup> To identify additional anti-inflammatory compounds from *Munronia* species, we performed a systematic investigation of the chemical constituents of *Munronia henryi* and screened them for anti-inflammatory activity. This study led to the isolation of three pimarane-type diterpenoids from *M. henryi*.

Pimarane diterpenoids are characterized by a 4, 4, 10, 13-tetramethylperhydrophenanthrene core skeleton and are classified into pimarane, isopimrane, *ent*-pimarane and *ent*-isopimrane based on their stereochemical configurations.<sup>9</sup> These compounds primarily occur in plants from the *Lamiaceae*, *Zingiberaceae*, and *Cupressaceae* families, as well as in fungi and marine organisms. To date, over 360 pimarane-type molecules have been reported, demonstrating notable cytotoxicity, anti-inflammatory, and antimicrobial activities.<sup>10</sup> However, such diterpenoids are rarely documented in Meliaceae plants, with only minor quantities isolated from *Dysoxylum*, *Guarea*, and *Chukrasia* species.<sup>11</sup> This study reports, for the first time, the presence of pimarane-type diterpenoids in *Munronia* plants, including compound 1, which features a unique 6,7-*seco* pimarane skeleton (Fig. 1). Additionally, their cytotoxic and anti-inflammatory activities are evaluated.

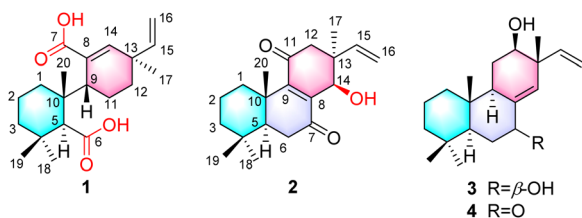


Fig. 1 The structures of compounds 1–4.

<sup>a</sup>, School of Pharmacy, Anhui University of Chinese Medicine, Anhui Province Key Laboratory of Bioactive Natural Products, Hefei 230012, P.R. China. E-mail: sunyp@ahtcm.edu.cn; wanggk@ahtcm.edu.cn

† Electronic supplementary information (ESI) available. ESI figures, biological assays, experimental and computational details, and original spectra (NMR, MS, UV, and ECD) of 1–3. CCDC 2452064. For ESI and crystallographic data in CIF or other electronic format see DOI: <https://doi.org/10.1039/d5ra04525h>

## Results and discussion

Compound 1 was obtained as a colorless square crystal, with a molecular formula of C<sub>20</sub>H<sub>30</sub>O<sub>4</sub>, as established by HR-ESI-MS (*m/z* 357.2046 [M + Na]<sup>+</sup>, calcd 357.2036), indicative of six degrees of unsaturation. The <sup>1</sup>H NMR spectrum (Table 1)



Table 1  $^1\text{H}$  NMR (600 MHz) and  $^{13}\text{C}$  NMR (150 MHz) data of compounds 1–3 ( $J$  in Hz)

No	$1^a$		$2^a$		$3^b$	
	$\delta_{\text{C}}$	$\delta_{\text{H}}$ ( $J$ in Hz)	$\delta_{\text{C}}$	$\delta_{\text{H}}$ ( $J$ in Hz)	$\delta_{\text{C}}$	$\delta_{\text{H}}$ ( $J$ in Hz)
1 $\alpha$	36.5	1.49, m <sup>c</sup>	35.0	0.96, dd (13.2, 3.7)	39.1	1.00, m
1 $\beta$		1.37, m		2.69, br d (13.2)		1.66, m
2 $\alpha$	19.8	1.50, m <sup>c</sup>	18.5	1.52, m	19.0	
2 $\beta$		1.62, m <sup>c</sup>		1.70, qt (13.7, 3.5)		1.48, m <sup>c</sup>
3 $\alpha$	42.0	1.19, m <sup>c</sup>	40.9	1.20, dd (13.6, 3.9)	41.9	1.17, td (13.3, 4.5)
3 $\beta$		1.53, m <sup>c</sup>		1.46, br d (13.4)		1.45, m <sup>c</sup>
4	34.5		33.1		33.3	
5	58.6	2.55, s	50.1	1.59, dd (15.0, 3.2)	52.0	3.87, t (8.0)
6 $\alpha$	177.1		35.7	2.56, dd (17.8, 3.2)	32.6	2.00, m
6 $\beta$				2.44, dd (17.8, 15.0)		1.29, m <sup>c</sup>
7	174.9		204.1		72.5	3.99, br s
8	135.3		141.1		139.4	
9	41.6	2.78, br s	156.0		50.3	1.93, m
10	42.7		39.4		38.4	
11 $\alpha$	21.5	1.60, m <sup>c</sup>	200.3		26.3	1.80, m
11 $\beta$		2.06, br d (14.7)				1.53, m
12 $\alpha$	33.8	1.54, m <sup>c</sup>	45.7	2.53, d (17.0)	73.2	3.57, dd (12.3, 3.9)
12 $\beta$		1.74, td (13.0, 3.0)		2.65, d (17.0)		
13	38.9		41.7		42.7	
14	144.7	6.33, s	68.9	4.55, d (2.6)	124.9	
15	147.1	5.73, dd (17.4, 10.6)	143.9	5.75, dd (17.6, 10.9)	146.2	5.80, dd (17.4, 10.8)
16a	112.7	4.82, d (17.6)	113.9	4.93, d (17.6)	114.1	5.14, d (17.4)
16b		4.96, d (10.6)		5.04, d (10.9)		5.15, d (10.8)
17	27.2	1.14, s	22.4	1.16, s	17.5	1.08, s
18	34.7	1.03, s	33.0	0.89, s	33.8	0.91, s
19	24.5	1.16, s	21.4	0.93, s	22.2	0.87, s
20	22.5	1.21, s	17.3	1.32, s	14.8	0.82, s

<sup>a</sup>  $^1\text{H}$  NMR (500 MHz) and  $^{13}\text{C}$  NMR (125 MHz) data in  $\text{CD}_3\text{OD}$ . <sup>b</sup>  $^1\text{H}$  NMR (600 MHz) and  $^{13}\text{C}$  NMR (150 MHz) data in  $\text{CDCl}_3$ . <sup>c</sup> overlapped.

showed the presence of four olefinic protons ( $\delta_{\text{H}}$  6.33, 1H, s; 5.73, 1H, dd,  $J = 17.4, 10.6$  Hz; 4.96, 1H, d,  $J = 10.6$  Hz; 4.82, 1H, d,  $J = 17.4$  Hz), and four tertiary methyl groups ( $\delta_{\text{H}}$  1.21, 1.16, 1.14 and 1.03, each 3H, s). Combined analysis of the  $^{13}\text{C}$  NMR and HSQC spectra (Table 1) exhibited 20 carbon signals, including four methyls, six methylenes (one olefinic at  $\delta_{\text{C}}$  112.7), four methines (two olefinic at  $\delta_{\text{C}}$  147.1, 144.7), six quaternary carbons (two carboxyls at  $\delta_{\text{C}}$  177.1, 174.9 and one olefinic at  $\delta_{\text{C}}$  135.3). The above data suggest that compound **1** contains one trisubstituted double bond, one terminal double bond, and four tertiary methyl groups, which are the characteristic fragments of pimarane-type diterpenoid.<sup>12</sup> However, the six degrees of unsaturation of compound **1** (accounting for two double bonds and two carboxyl groups) imply the presence of only two rings in its structure. Additionally, the two carboxyl groups indicate that the pimarane skeleton of compound **1** has undergone ring-opening.

The 2D NMR spectra revealed key structural features of compound **1** (Fig. 2). In the HMBC spectrum, H<sub>3</sub>-18 ( $\delta_{\text{H}}$  1.03, 3H, s) showed correlations to C-19 ( $\delta_{\text{C}}$  24.5), C-3 ( $\delta_{\text{C}}$  42.0), C-4 ( $\delta_{\text{C}}$  34.5), and C-5 ( $\delta_{\text{C}}$  58.6). These correlations, together with the  $^1\text{H}$ - $^1\text{H}$  COSY cross-peaks between H-1/H-2/H-3, confirmed the intact nature of ring A. Furthermore, HMBC correlations of H<sub>3</sub>-17 ( $\delta_{\text{H}}$  1.14, s) to C-12 ( $\delta_{\text{C}}$  33.8) and C-14 ( $\delta_{\text{C}}$  144.7), along with those of H-14 ( $\delta_{\text{H}}$  6.33, s) to C-9 ( $\delta_{\text{C}}$  41.6) and C-12, combined

with the  $^1\text{H}$ - $^1\text{H}$  COSY cross-peaks of H-9/H-11/H-12, established the complete ring C structure. Furthermore, the HMBC correlations between H-14 and  $\delta_{\text{C}}$  174.9, and between H-5 and  $\delta_{\text{C}}$  177.1 suggested that the two carboxyl groups belong to C-7 and C-6, respectively. This assignment was further supported by the molecular formula derived from HR-MS analysis. Consequently, compound **1** was identified as a 6,7-*seco* pimarane-type diterpenoid, as illustrated in the Fig. 1. Notably, the  $^{13}\text{C}$  NMR spectrum of **1** exhibits signal broadening, likely attributable to steric hindrance from the carboxyl group restricting free rotation about the C9–C10 single bond.<sup>13</sup>

The relative configuration of compound **1** was partially established through ROESY correlations (Fig. 2). The cross-peaks between H<sub>3</sub>-18/H-5/H-3 $\alpha$  indicated  $\alpha$ -orientation for

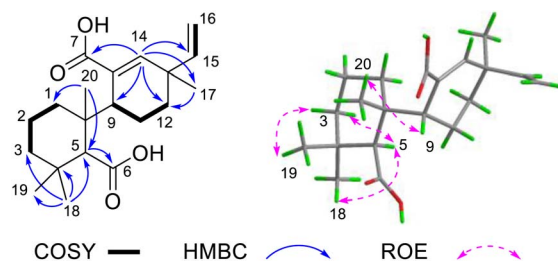


Fig. 2 Key 2D NMR correlations of **1**.



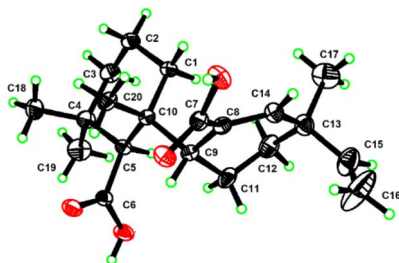


Fig. 3 X-ray structure of **1**.

both H<sub>3</sub>-18 and H-5, while the correlation between H<sub>3</sub>-19 and H-3β supported β-orientation for H<sub>3</sub>-19. However, the stereo-configuration of compound **1** could not be determined by ROESY due to the free rotation about the C9–C10 single bond. The absolute configuration was ultimately determined by X-ray crystallographic analysis of single crystals (Fig. 3) obtained from methanol solution, which established the 5*S*, 9*R*, 10*R*, 13*R* configuration [Flack parameter = −0.06(13)].

Compound **2** was obtained as a white powder. Its molecular formula was established as C<sub>20</sub>H<sub>28</sub>O<sub>3</sub> by HR-ESI-MS (*m/z* 315.1960 [M – H]<sup>−</sup>), corresponding to seven degrees of unsaturation. The <sup>1</sup>H NMR spectrum of **2** (Table 1) displayed signals characteristic of a terminal double bond (δ<sub>H</sub> 5.75, dd, *J* = 17.6, 10.9 Hz; 5.04, d, *J* = 10.9 Hz; 4.93, d, *J* = 17.6 Hz) and four tertiary methyl groups (δ<sub>H</sub> 1.32, 1.16, 0.93 and 0.89, each 3H, s). The <sup>13</sup>C spectrum of **2**, combined with the HSQC spectrum, revealed the presence of seven quaternary carbons (including two keto carbonyls at δ<sub>C</sub> 204.1 and 200.3, and two olefinic carbons at δ<sub>C</sub> 156.0 and 141.4), three methine carbons (one olefinic at δ<sub>C</sub> 143.9, and one oxygenated at δ<sub>C</sub> 69.0), six methylene carbons (one olefinic at δ<sub>C</sub> 113.9) and four methyl carbons. These signals account for four degrees of unsaturation, while the remaining three unsaturations suggest that **2** is a tricyclic diterpenoid. The spin systems identified in the <sup>1</sup>H–<sup>1</sup>H COSY spectrum (Fig. 4), specifically H-1/H-2/H-3 and H-5/H-6, along with key HMBC correlations (H<sub>3</sub>-18 to C-3/C-4/C-5; H-20 to C-1/C-5/C-9/C-10; and H-6 to C-7/C-8/C-10), were crucial for establishing the structures of rings A and B. Combined with the terminal double bond feature and HMBC correlations from H-17 to C-12, C-14, C-15, compound **2** was identified as a pimarane-type diterpenoid, exhibiting a planar structure similar to known compound 12β-Hydroxy-7,11-dioxopimar-8,15-dien.<sup>14</sup> The sole structural difference involves the position of hydroxyl group substitution in **2**, the hydroxyl group is located at C-14,

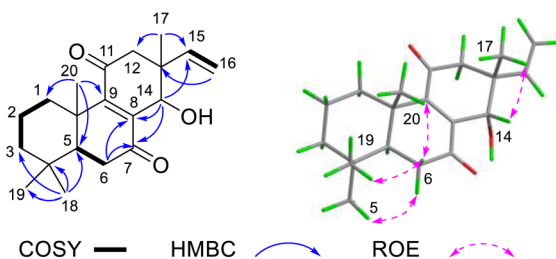


Fig. 4 Key 2D NMR correlations of **2**.

whereas in 12β-hydroxy-7,11-dioxopimar-8,15-dien, it is positioned at C-12. This distinction was confirmed by the HMBC correlations observed between H-14 and C-7/C-8.

The ROESY spectrum revealed key spatial relationships: correlations between H<sub>3</sub>-19 (δ<sub>H</sub> 0.93), H-6β (δ<sub>H</sub> 2.44), H<sub>3</sub>-20 (δ<sub>H</sub> 2.69) indicated their cofacial arrangement and β-orientation. Similarly, the H<sub>3</sub>-18 (δ<sub>H</sub> 0.89)/H-6α (δ<sub>H</sub> 2.56) correlation suggested their cofacial α-orientation (Fig. 4). The α-orientation of H-5 was further supported by its small coupling constant (*J*<sub>5,6α</sub> = 3.2 Hz). While the ROESY correlation between H<sub>3</sub>-17 (δ<sub>H</sub> 1.16) and H-14 (δ<sub>H</sub> 4.55) confirmed their cofacial arrangement, two possible relative configurations (13*S*\*, 14*R*\* and 13*R*\*, 14*S*\*) remained. To resolve this ambiguity, we calculated the <sup>13</sup>C chemical shifts for both epimers (Fig. 5A). DP4+ analysis of both <sup>1</sup>H and <sup>13</sup>C NMR data unequivocally identified (13*S*\*, 14*R*\*)-**2** as the correct structure (100% probability, Fig. S3†).<sup>15,16</sup> The absolute configuration (5*S*, 10*S*, 13*S*, 14*R*) was ultimately confirmed by excellent agreement between experimental and calculated ECD spectra (Fig. 5B).

Compound **3** was isolated as a white powder. Its molecular formula (C<sub>20</sub>H<sub>32</sub>O<sub>2</sub>) was established by <sup>13</sup>C NMR and HR-ESI-MS (observed [M – H]<sup>−</sup> at *m/z* 327.2295), implying five degrees of unsaturation. The <sup>1</sup>H NMR spectrum (Table 1) displayed characteristic methyl group signals (δ<sub>H</sub> 1.08, 0.91, 0.87, 0.82, each, 3H, s) and olefinic proton signals (δ<sub>H</sub> 5.80, dd, *J* = 17.4, 10.8 Hz; 5.54, d, *J* = 2.0 Hz; 5.15, d, *J* = 10.8 Hz; 5.14, d, *J* = 17.4 Hz), suggesting a pimarane-type diterpenoid skeleton analogous to compound **2**. Comparative analysis of 1D and 2D NMR data revealed close structural similarity to (5*S*, 9*R*, 10*S*, 12*R*, 13*R*)-12-hydroxyisopimara-8(14),15-dien-7-one,<sup>17</sup> with only differences of the absence of a carbonyl carbon and the presence of an

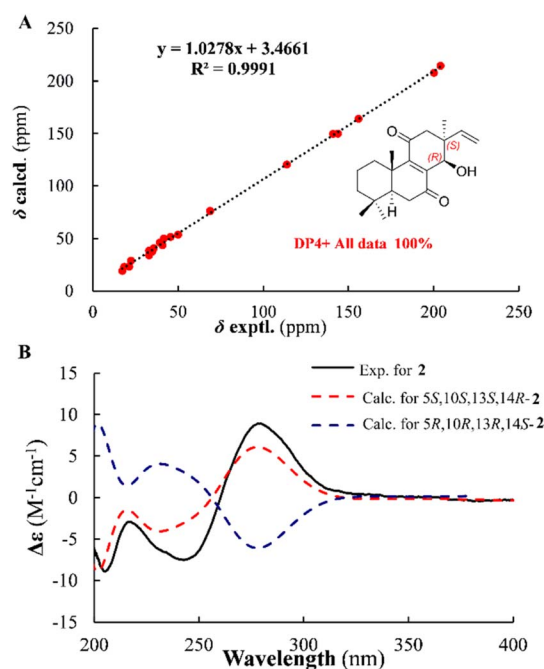


Fig. 5 Correlations between experimental and calculated <sup>13</sup>C NMR chemical shifts of (13*S*\*, 14*R*\*)-**2** (A) and ECD calculations for (13*S*, 14*R*)-**2** (B).



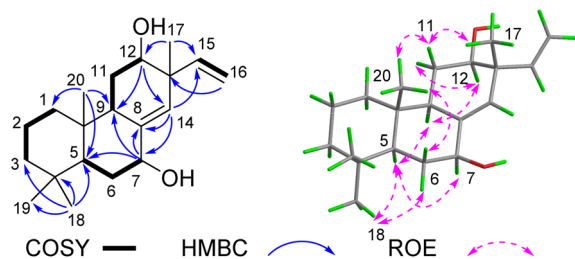


Fig. 6 Key 2D NMR correlations of **3**.

additional oxygenated carbon. The observed mass difference of 2 suggested reduction of the C-7 carbonyl group to a hydroxyl group in compound **3**. This structural modification was confirmed by HMBC correlations from H-7 ( $\delta_{\text{H}}$  3.99) to C-5 ( $\delta_{\text{C}}$  52.0), C-8 ( $\delta_{\text{C}}$  139.4), C-9 ( $\delta_{\text{C}}$  50.3), along with  $^1\text{H}$ - $^1\text{H}$  COSY cross-peaks between H-5/H-6/H-7 (Fig. 6).

ROESY correlations observed among H<sub>3</sub>-18/H-5/H-9/H-12, H-5/H-7, and H<sub>3</sub>-18/H-6 $\alpha$  ( $\delta_{\text{H}}$  2.00) established their cofacial arrangement and  $\alpha$ -orientation. Complementary ROESY cross-peaks between H<sub>3</sub>-17/H-11 $\beta$  ( $\delta_{\text{H}}$  1.53)/H<sub>3</sub>-20/H-6 $\beta$  ( $\delta_{\text{H}}$  1.29) confirmed their  $\beta$ -orientation. The absolute configuration of **3** was determined to be 5*S*, 7*S*, 9*R*, 10*S*, 12*R*, 13*R* through comparison of experimental and calculated ECD spectra (Fig. S2 $\dagger$ ).

In addition to the aforementioned compounds, a known pimarane-type diterpenoid was isolated from *M. henryi*. Based on comparison of its spectroscopic data with literature values,<sup>17</sup> this compound was identified as (5*S*, 9*R*, 10*S*, 12*R*, 13*R*)-12-hydroxyisopimara-8(14),15-dien-7-one (**4**).

According to previous literature, pimarane-type diterpenoids have demonstrated significant cytotoxic and anti-inflammatory potential.<sup>18–20</sup> Initially, all compounds were tested for anti-inflammatory activity using L-NMMA (50  $\mu\text{M}$ ) as a positive control (52.75  $\pm$  1.28% inhibition). At 50  $\mu\text{M}$  concentration, compounds **1–4** exhibited no significant inhibitory effects on NO production in LPS-induced RAW 264.7 macrophages, showing inhibition rates ranging from 13.73% to 32.35%.

Subsequently, the cytotoxicity of these compounds was evaluated against human colon cancer cells (HCT-166) and human liver cancer cells (Hep3B). None of the compounds exhibited significant cytotoxicity against either cancer cell line.

## Conclusions

In summary, four pimarane-type diterpenoids were isolated from the petroleum ether extract of *Munronia henryi*, including three previously undescribed compounds (**1–3**) and one known analogue. Muhenrin A (**1**) features a novel 6,7-*seco* pimarane skeleton, likely biosynthesized from 7 $\alpha$ -hydroxyisopimara-8(14),15-diene.<sup>21</sup> Two possible pathways are proposed for its formation (Scheme S1 $\dagger$ ). Path a: the 7-hydroxyl group of 7 $\alpha$ -hydroxyisopimara-8(14),15-diene is oxidized to a ketone carbonyl (i), followed by Baeyer–Villiger oxidation to yield the lactone intermediate (ii).<sup>22</sup> Subsequent hydrolysis and continuous oxidation produce **1**. Path b: 7 $\alpha$ -hydroxyisopimara-8(14),15-diene undergoes dehydration to form the alkene

intermediate (iv), which is then directly oxidized to **1** via dioxygenase activity.<sup>23</sup> To our knowledge, this represents the first report of pimarane-type diterpenoids from *Munronia* species.

The initial biological activity assays did not yield significant results. Future studies should consider alternative cell models or explore additional biological activities, such as antibacterial or antiviral effects.<sup>24,25</sup>

## Experimental

### General experimental procedures

Optical rotations were measured with a P-2000 digital polarimeter (solvent: MeOH, JASCO, Japan). UV spectra were obtained on a UV-2401A spectrophotometer (solvent: MeOH, Shimadzu, Japan). Circular dichroism (CD) spectra were obtained on a JASCO(J-1500) CD spectrometer in MeOH (Applied Photophysics, Japan). HRMS-ESI was performed on a Thermo Orbitrap Exploris 120 mass spectrometer (Thermo Fisher Scientific, USA, Xevo G2 - XSQT of mass spectrometer from Waters, USA). In addition, 1D and 2D NMR spectra were recorded on Bruker DRX-500 and 600 spectrometers (Bruker, Germany) at 298 K (internal standard: TMS, solvent: CD<sub>3</sub>OD and CDCl<sub>3</sub>). Silica gel (200–300 mesh, Qingdao Haiyang, China), Sephadex LH-20 (GE, USA), and RP-18 (5  $\mu\text{m}$ , Fuji Silysia Chemical, Japan) were used for column chromatography. MPLC was performed on a Büchi Sepacore System equipped with a pump manager (Büchi, Switzerland) and prep-HPLC was performed on a 1260 instrument (Agilent, USA).

### Plant material

The whole plant of *Munronia henryi* was collected in November 2022 from Wenshan Zhuang and Miao Autonomous Prefecture, Yunnan province, P. R. China, and identified by Professor Qing-Shan Yang of Anhui University of Chinese Medicine. A voucher specimen (no. 20221101) was deposited in the Department of Traditional Chinese Medicine and Natural Medicinal Chemistry at Anhui University of Chinese Medicine.

### Extraction and isolation

The dried and pulverized aerial parts of *Munronia henryi* (20 kg) were exhaustively extracted with 95% ethanol (4  $\times$  3 h, reflux). The combined ethanolic extracts were concentrated under reduced pressure to yield a crude extract, which was subsequently suspended in H<sub>2</sub>O and partitioned with dichloromethane (DCM). The DCM portion was suspended in water and then extracted with petroleum ether (PE).

The PE fraction (363 g) was fractionated by silica gel column chromatography using a stepwise gradient of PE-EtOAc (100 : 0  $\rightarrow$  0 : 100, v/v) to yield eight fractions (A–H). Fraction F (27.1 g) was further purified by ODS column chromatography with a MeOH–H<sub>2</sub>O gradient (40 : 60  $\rightarrow$  100 : 0, v/v), yielding six sub-fractions (Fa–Ff). Subfraction Fc was chromatographed on ODS with isocratic elution (MeCN–H<sub>2</sub>O, 45 : 55, v/v) to afford nine fractions (Fca–Fci). Final purification of Fcc by semi-preparative HPLC (MeCN–H<sub>2</sub>O, 65 : 35, 8.0 mL min<sup>-1</sup>) yielded compound **4** (4.81 mg,  $t_{\text{R}}$  = 36 min).



Similarly, subfraction Fb was separated by ODS chromatography (isocratic MeCN–H<sub>2</sub>O, 45 : 55) into thirteen fractions (Fba–Fbn). Fraction Fbk was purified by semi-preparative HPLC (MeCN–H<sub>2</sub>O 57 : 43, 8.0 mL min<sup>-1</sup>) to give Fbka (4.71 mg, *t*<sub>R</sub> = 43 min), which was further purified (MeOH–H<sub>2</sub>O, 75 : 25, 8.0 mL min<sup>-1</sup>) to afford compound 3 (2.58 mg, *t*<sub>R</sub> = 28 min). Fraction Fbn was processed similarly (MeCN–H<sub>2</sub>O, 67 : 33 → MeOH–H<sub>2</sub>O, 55 : 45) to yield compound 2 (2.55 mg, *t*<sub>R</sub> = 32 min) *via* intermediate fraction Fbna (5.31 mg, *t*<sub>R</sub> = 45 min).

Fraction H (24.2 g) was fractionated by MCI gel column chromatography using a MeOH–H<sub>2</sub>O gradient (20 : 80 → 100 : 00, v/v), yielding six subfractions (Ha–Hf). Subfraction Hf was further purified by Sephadex LH-20 column chromatography (MeOH) to afford four fractions (Hfa–Hfd). Final purification of Hfb by semi-preparative HPLC (MeCN–H<sub>2</sub>O gradient: 0–30 min, 55 : 45; 30–35 min, 55 : 45 → 85 : 15; 35–50 min, 85 : 15; flow rate 8.0 mL min<sup>-1</sup>) yielded compound 1 (6.75 mg, *t*<sub>R</sub> = 43 min).

**Muhenrin A (1).** Colorless square crystal; [ $\alpha$ ]<sub>D</sub><sup>25</sup> – 53.0 (*c* = 0.2, MeOH); UV  $\lambda_{\max}$  (MeOH) nm (log  $\epsilon$ ): 210 (4.62); ECD (MeOH)  $\lambda_{\max}$  ( $\Delta\epsilon$ ) 237.5(+16.72) nm; IR (KBr) cm<sup>-1</sup> 3457, 2951, 2864, 2831, 1701, 1604, 1448, 1365, 1227, 1205, 1152; <sup>1</sup>H and <sup>13</sup>C NMR data see Table 1; HRESI-MS *m/z* 357.2046[M + Na]<sup>+</sup> (calcd for 357.2036, C<sub>20</sub>H<sub>30</sub>O<sub>4</sub>Na).

**Muhenrin B (2).** White powder; [ $\alpha$ ]<sub>D</sub><sup>25</sup> – 2.9 (*c* 0.31, MeOH); UV (MeOH)  $\lambda_{\max}$  (log  $\epsilon$ ) 239 (2.24) nm; ECD (MeOH)  $\lambda_{\max}$  ( $\Delta\epsilon$ ) 205(–8.87) nm, 217 (–2.92) nm, 242 (–7.5) nm, 279 (+8.9) nm; IR (KBr) cm<sup>-1</sup> 3394, 2922, 2831, 2716, 1600, 1364, 1154, 1068, 971, 775; <sup>1</sup>H and <sup>13</sup>C NMR data see Table 1; HR-ESI-MS *m/z* 315.1960 [M – H]<sup>–</sup> (calcd for 315.1955, C<sub>20</sub>H<sub>27</sub>O<sub>3</sub>).

**Muhenrin C (3).** White powder; [ $\alpha$ ]<sub>D</sub><sup>25</sup> + 10.3 (*c* 0.13, MeOH); UV (MeOH)  $\lambda_{\max}$  (log  $\epsilon$ ) 210 (3.12) nm; ECD (MeOH)  $\lambda_{\max}$  ( $\Delta\epsilon$ ) 299 (+0.48) nm; IR (KBr) cm<sup>-1</sup> 3394, 2922, 2831, 2716, 1600, 1364, 1154, 1068, 971, 775; <sup>1</sup>H and <sup>13</sup>C NMR data see Table 1; HR-ESI-MS *m/z* 327.2295[M + Na]<sup>+</sup> (calcd for 327.2294, C<sub>20</sub>H<sub>32</sub>O<sub>2</sub>Na).

**Crystal data for muhenrin A (1).** C<sub>20</sub>H<sub>30</sub>O<sub>4</sub>, *M* = 334.44, *a* = 12.0825(8) Å, *b* = 12.7004(8) Å, *c* = 12.9052(8) Å,  $\alpha$  = 90°,  $\beta$  = 90°,  $\gamma$  = 90°, *V* = 1980.3(2) Å<sup>3</sup>, *T* = 170.0 K, space group *P*<sub>2</sub><sub>1</sub>, *Z* = 4,  $\mu$ (Cu K $\alpha$ ) = 0.613 mm<sup>-1</sup>, 17 312 reflections measured, 3988 independent reflections (*R*<sub>int</sub> = 0.0736). The final *R*<sub>1</sub> values were 0.0582 (*I* > 2 $\sigma$ (*I*)). The final  $wR$ (*F*<sup>2</sup>) values were 0.1559 (*I* > 2 $\sigma$ (*I*)). The final *R*<sub>1</sub> values were 0.0621 (all data). The final  $wR$ (*F*<sup>2</sup>) values were 0.1622 (all data). The goodness of fit on *F*<sup>2</sup> was 1.019. Flack parameter = –0.06(13). A suitable crystal was selected and recorded with a diffractometer using Cu K $\alpha$  radiation. The structure was solved with the ShelXT structure solution program using direct methods and refined with the ShelXL refinement package using least squares minimisation based on Olex2 software. The crystallographic data of compounds have been deposited at the Cambridge Crystallographic Data Center with the deposition number CCDC 2452064 (1).

## Data availability

The data supporting this article have been included as part of the ESI.† Crystallographic data for muhenrin A (1) has been

deposited at the CCDC under 2452064 and can be obtained from <https://www.ccdc.cam.ac.uk/>

## Conflicts of interest

There are no conflicts to declare.

## Acknowledgements

This work was partially supported by the National Natural Science Foundation of China (32400324), the Natural Science Key Research Program of Anhui Province University (2022AH050489), the Foundation of Anhui Province Key Laboratory of Research & Development of Chinese Medicine (AKLPDCM202305), the Open Fund of High-level Key Discipline of Chemistry of Chinese Medicine of the State Administration of Traditional Chinese Medicine, Anhui University of Chinese Medicine (HKDCCM2024013), and the Anhui Province University Discipline (Professional) Leader Training Project (DTR2023026).

## Notes and references

- 1 *Flora Reipublicae Popularis Sinicae*, ed. Editorial Committee of FRPS, Science Press, Beijing, 1997, vol. 43(3), p. 57.
- 2 Y. Yan, J.-X. Zhang, T. Huang, X.-Y. Mao, W. Gu, H.-P. He, Y.-T. Di, S.-L. Li, D.-Z. Chen, Y. Zhang and X.-J. Hao, *J. Nat. Prod.*, 2015, **78**(4), 811–821.
- 3 X.-R. Yang, N. Tanaka, D. Tsuji, F.-L. Lu, X.-J. Yan, K. Itoh, D.-P. Li and Y. Kashiwada, *Tetrahedron*, 2019, **75**, 130779.
- 4 Y. Yan, D. Wang, X. Zhang, M.-Y. Peng, X.-Y. Yan, Y.-S. Guo, M.-G. Jia, J. Zhou, L. Tang and X.-J. Hao, *Pestic. Biochem. Physiol.*, 2022, **184**, 105108.
- 5 X.-R. Yang, P.-y. Liu, Y.-L. Wei, J.-R. Song, X.-J. Yan, X.-H. Jiang, J.-X. Li, X.-Q. Li, D. P. Li and F.-L. Lu, *Molecules*, 2023, **28**, 6839.
- 6 Y.-P. Sun, Q.-R. Li, L.-T. Cui, P.-F. Tang, Y.-Y. Li, L.-Y. Kong and J. Luo, *Chin. J. Chem.*, 2022, **40**, 123–136.
- 7 Y.-P. Sun, L.-T. Cui, Q.-R. Li, P.-F. Tang, Y.-Y. Li, W.-J. Xu, J. Luo and L. Y. Kong, *Chin. Chem. Lett.*, 2022, **33**, 516–518.
- 8 Y.-P. Sun, Q. R. Li, Y. J. Sun, L. T. Cui, Y.-Y. Wang, Y.-Y. Li, J. Luo and L. Y. Kong, *J. Nat. Prod.*, 2021, **84**, 2352–2365.
- 9 K. Ye and H. Ai, *Pharmaceuticals*, 2022, **15**, 1291.
- 10 H. Q. Zhang, M. Li, A. Lvha and S.-M. Zhang, *Nat. Prod. Res.*, 2024, DOI: [10.1080/14786419.2024.2426071](https://doi.org/10.1080/14786419.2024.2426071).
- 11 N. A. Najihah, W. Safriansyah, S. E. Sinaga, M. A. Nafiah and U. Supratman, *Phytochem. Rev.*, 2025, DOI: [10.1007/s11101-025-10110-z](https://doi.org/10.1007/s11101-025-10110-z).
- 12 J. Boonsombat, C. Mahidol, P. Chawengrum, N. Reuk-Ngam, N. Chimnoi, S. Techasakul, S. Ruchirawat and S. Thongnes, *Phytochemistry*, 2017, **143**, 36–44.
- 13 P. Zhang, S. Xue, W. Huang, C. Wang, Z. Cui, J. Luo and L. Kong, *Org. Chem. Front.*, 2021, **8**, 566–571.
- 14 A. C. Pinto and C. Borges, *Phytochemistry*, 1983, **22**(9), 2011–2015.
- 15 M. W. Lodewyk, M. R. Siebert and D. J. Tantillo, *Chem. Rev.*, 2012, **112**, 1839–1862.



- 16 N. Grimblat, M. M. Zanardi and A. M. Sarotti, *J. Org. Chem.*, 2015, **80**, 12526–12534.
- 17 K. Jiang, L.-L. Chen, S.-F. Wang, Y. Wang, Y. Li and K. Gao, *J. Nat. Prod.*, 2015, **78**(5), 1037–1044.
- 18 Y.-Y. Chen, X.-T. Zeng, D.-Q. Xu, S.-J. Yue, R.-J. Fu, X. Yang, Z.-X. Liu and Y.-P. Tang, *Phytochemistry*, 2022, **197**, 113113.
- 19 H.-B. Yu, X.-L. Wang, Y.-X. Zhang, W.-H. Xu, J.-P. Zhang, X.-Y. Zhou, X.-L. Lu, X.-Y. Liu and B.-H. Jiao, *J. Nat. Prod.*, 2018, **81**(7), 1553–1560.
- 20 K. Xu, X. Zhang, J. W. Chen, Y. Shen, N. Jiang, R. X. Tan, R. H. Jiao and H. M. Ge, *Tetrahedron Lett.*, 2019, **60**(38), 151045.
- 21 E. M. G. Touchè, E. G. Lopez, A. P. Reyes, H. Sánchez, F. Honecker and H. Achenbach, *Phytochemistry*, 1997, **45**, 387.
- 22 V. Dorado, C. I. Herrerías and J. M. Fraile, *Tetrahedron*, 2023, **139**, 133450.
- 23 J. Zou, J. Ye, C. Zhao, J. Zhang, Y. Liu, L. Pan, K. He and H. Zhang, *Int. J. Mol. Sci.*, 2023, **24**(17), 13451.
- 24 J. Boonsombat, C. Mahidol, P. Chawengrum, N. Reuk-Ngam, N. Chimnoi, S. Techasakul, S. Ruchirawat and S. Thongnest, *Phytochemistry*, 2017, **143**, 36–44.
- 25 Y. P. Tan, Y. Xue, A. I. Savchenko, S. D. Houston, N. Modhiran, C. L. D. McMillan, G. M. Boyle, P. V. Bernhardt, P. R. Young, D. Watterson and C. M. Williams, *J. Nat. Prod.*, 2019, **82**(10), 2828–2834.

